Impact of high ionospheric activity on GPS surveying: Experiences from the Hellenic RTK-network during 2011-12

M. Gianniou, E. Mitropoulou
Geodetic Department
KTIMATOLOGIO S.A. (Hellenic Cadastre), 288 Mesogion Ave., 15562 Holargos, Athens, Greece

Abstract. GNSS is being increasingly used for surveying and other high precision applications. GNSS users prefer RTK than post-processing as RTK minimizes the occupation time and does not require trained personnel to process the observations. However, RTK is much more sensitive to unfavorable observation conditions, like poor satellite geometry, multipath, electromagnetic interferences and active ionosphere. Such conditions can cause significant performance degradation of RTK, i.e. reduced accuracy, long initialization time or even inability to obtain a fixed solution. Among the various error sources, ionosphere is the most difficult to mitigate, particularly during periods of high solar activity.

Since 2011 users of HEPOS, the Hellenic RTK-network, often need longer initialization times than in the previous years. Sometimes, initialization can hardly be achieved. Such difficulties were expected as we are approaching the maximum of the 24th solar cycle. Furthermore, Greece lies in the southernmost part of Europe (lowest latitude is less than 35°) and the ionospheric effects are rather intense. Values of the Ionospheric Index I_{95} higher than 30 have been observed in HEPOS in 2011. In order to assess the impact of the ionospheric activity on the performance of different GNSS techniques we analyzed several data including RTK and post-processed measurements both from physical and virtual reference stations. The initialization time and the achieved precision and accuracy were examined with respect to the ionospheric activity. Comparison of measurements conducted on the same points with the same satellite geometry but under different ionospheric conditions showed that high ionospheric activity can increase dramatically the initialization time and deteriorate significantly the achievable accuracy. The paper discusses the observations used, the processing schemes and the obtained results.

Keywords. GPS-RTK, ionospheric disturbances, I_{95} index, 24th solar cycle, Greece, HEPOS.

1 Introduction

Generally speaking, the ionosphere is the main limiting parameter in geodetic relative GPS positioning. In order to deal with the errors caused by the ionospheric refraction dual frequency receivers are used. When using single frequency receivers the baseline length is limited to about 5-10km, depending on the ionospheric conditions. Under intense ionospheric conditions even dual frequency receivers cannot ensure efficient and accurate positioning: Longer observation time may be needed to resolve the carrier-phase ambiguities, the baseline length for effective positioning is being reduced and the accuracy is being degraded.

The level of charge of the ionosphere is usually described using TEC (Total Electron Content). TEC represents the total number of electrons between a satellite and a receiver on earth, along a tube of one squared meter cross section. TEC is measured in TEC Units (TECU), where 1 TECU = 10^{16} electrons/m². TEC is influenced by the solar activity, diurnal and seasonal variations and the earth's magnetic field (Hofmann-Wellenhof et al. 2008). The geographic distribution of TEC depends strongly on the geomagnetic latitude. As shown in Figure 1, three kinds of regions are distinguished (Warnant et al, 2003):

- The mid-latitude regions where TEC and its gradients are the lowest and most regular
- The equatorial region where the highest TEC gradients and TEC values are observed
- The polar regions where TEC is mostly variable and irregular and its behaviour strongly depends on geomagnetic activity.

For a southern country like Greece the dependency of TEC on geomagnetic latitude is particularly important. As can be seen in Figure 1 the southern part of the country (mainly Crete) is considered to belong to the equatorial region. The higher ionospheric activity in southern Greece can be seen in Figure 2 which gives a representative example of the spatial distribution of TEC in

Europe. The impact of the high ionospheric activity on GPS positioning in Greece -and particularly on Crete-will be demonstrated in section 4.2.

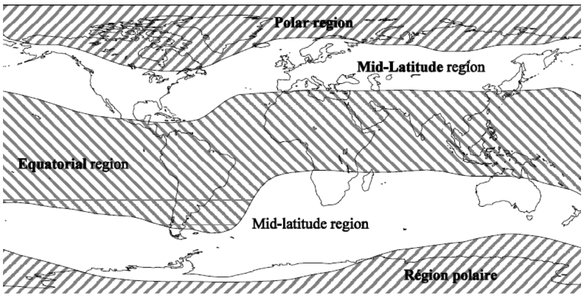

Fig. 1 Ionospheric activity and geomagnetic latitude *(source: Warnant et al, 2003).*

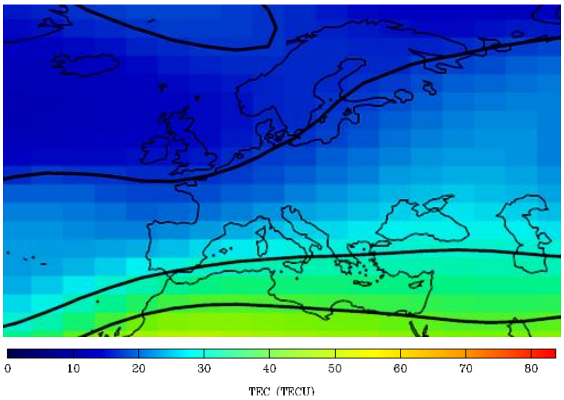

Fig. 2 Typical spatial distribution of TEC over Europe on May 2, 2012 14:00 UT (CODE'S GIM).

2 Ionospheric activity approaching the maximum of the 24th solar cycle

As known, the ionospheric activity follows the solar cycle, a nearly periodic 11-year variation in the activity of the Sun. Solar activity is a general term which can refer a) to the intensity of the solar electromagnetic radiation and b) to solar events like coronal mass ejections (CME) and solar proton events (Liu et al., 2011). There are several ways to quantify the solar activity like the sunspot number (SSN) and the TEC. Figure 3 depicts the variation in SSN during the last 36 years. TEC information can be given in form of Global Ionospheric Map (GIM) (see e.g. Figure 2) or, in a more comprehensive way, using Mean TEQ (Schaer, 1999). Mean TEC can be used to easily obtain an overview of the evolution of the solar activity on a global level. Figure 4 shows the Mean TEC values computed from GNSS observations at the Centre for Orbit Determination in Europe (CODE). Daily values, interpolation and a trend function are given. Details about the prediction procedure can be found in Schaer et al. (1998). The increase of ionospheric activity is obvious as we are approaching the maximum of the 24th solar cycle.

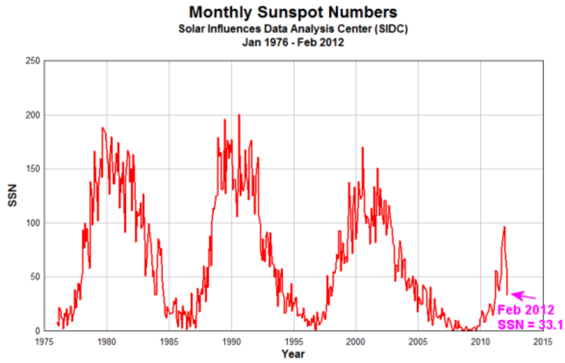

Fig. 3 Monthly Sunspot Numbers for the time period Jan. 1976 to Feb. 2012 (*data source: Royal Observatory of Belgium, www.sidc.be*).

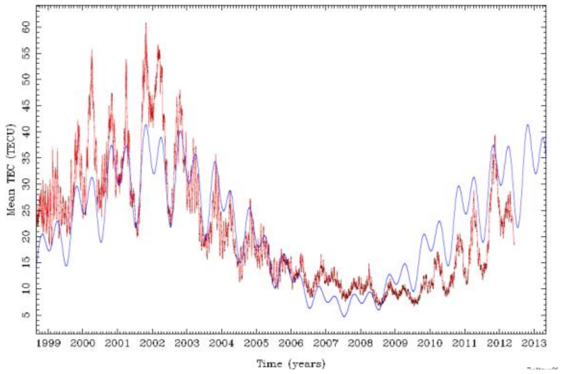

Fig. 4 Daily Mean TEC values (in TECU) (black dots), interpolation (red curve) and a trend function (blue curve) for the time period September 1999 to May 2012 *(source: CODE).*

3 Ionospheric activity and network-RTK

Typically, under normal atmospheric conditions single-base RTK is effective for distances up to 20-30 km between the rover receiver and the reference station. During periods of high solar activity larger TEC values, larger TEC gradients and a larger number of ionospheric disturbances are observed (Warnant et al., 2003). Depending on the intensity of the ionospheric activity the effectiveness of single-base RTK is considerably degraded. In the case of a network of GNSS reference stations the ionospheric error is being modeled, so network-

RTK is considerably less affected by the ionosphere than single-base RTK. Due the high importance of the ionospheric error the I_{95} index has been introduced, which provides statistical information on expected residual ionospheric biases within the area of a GNSS network (Wanninger, 1999). The I_{95} index is based on the coefficients ΔI_{LAT} and ΔI_{LON} which represent the differential ionospheric biases in the south-north and east-west directions, respectively. Based on these two coefficients the following quantity is being computed:

$$\Delta I = \sqrt{\Delta I_{LAT}^2 + \Delta I_{LON}^2} \qquad (1)$$

The I_{95} index is defined as the 95% margin of all ΔI values in a pre-defined interval of time (Wanninger, 2004). In most networks (also in HEPOS) this time interval is set to one hour. I_{95} index values do not only depend on the ionospheric conditions but also on several other factors, like reference station distances and elevation mask. However, in most networks an elevation mask of about 10^o is being used and the stations are located at distances between 50 km and 80 km, so the I_{95} values of different networks are more or less comparable. For the interpretation of the I_{95} values Wanninger (2004) suggested three thresholds values (2, 5 and 10) as follows:

- $I_{95} \leq 2$: low electron content and undisturbed ionospheric conditions
- $2 \leq I_{95} \leq 5$: high electron content but no irregularities
- I_{95} values of 10 or even more: medium-scale disturbances, whereas small-scale disturbances can cause even larger values.

Similar values are used in networking software packages. For instance GPSNet software uses the following three values to classify ionospheric activity (Trimble (2008):

- $I_{95} \leq 2$: low activity (undisturbed ionosphere)
- $2 \leq I_{95} \leq 5$: medium activity
- $I_{95} \geq 8$: high activity.

Figure 5 gives the I_{95} plot of HEPOS network for December 6, 2011. Values clearly above 8 indicate high ionospheric activity. Such plots become very common since the end of 2011 as we are approaching the maximum of 24^{th} solar cycle.

Another indicator of ionospheric linearity is IRIU (Ionospheric Residual Interpolation Uncertainty). IRIU is computed based on the RMS of the interpolation of the ionospheric biases, so it expresses how good the interpolation is (Chen et al., 2003). For this reason IRIU provides to the users of RTK-networks valuable information on the expected RTK performance at any location within the network for a given time. Figures 6 and 7 depict IRIU values for the network BLVA in Germany at GPS time 07:00 and 08:45, respectively. Comparing

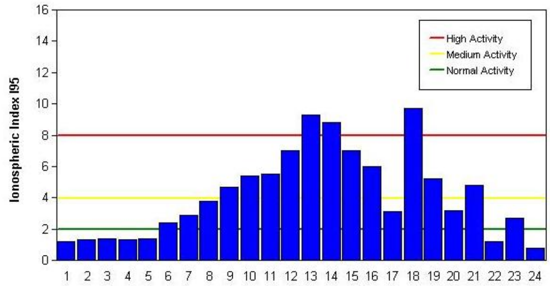

Fig. 5 I_{95} plot of HEPOS network for Dec. 6, 2011.

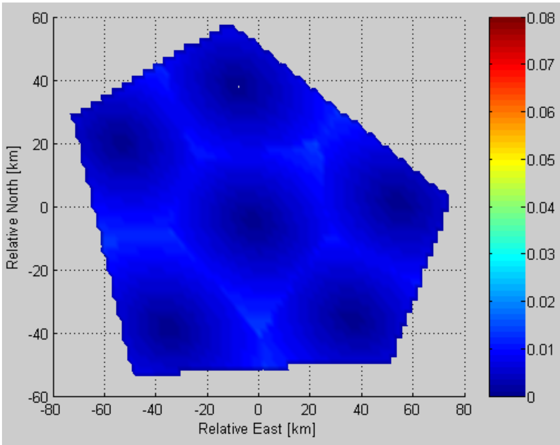

Fig. 6 IRIU at GPS time 07:00 of BLVA network (source: Chen et al., 2003).

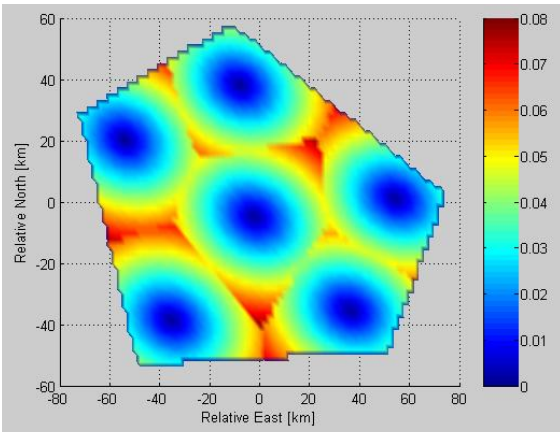

Fig. 7 IRIU at GPS time 08:45 of BLVA network (source: Chen et al., 2003).

Figures 6 and 7 it becomes obvious that the uncertainty of the ionospheric parameters within the network increases around noon as solar radiation increases. Moreover, Figure 7 clearly indicates that the IRIU becomes higher at points away from the reference stations.

4 Data analysis

In order to assess the impact of increased ionospheric activity on RTK positioning, different tests have been made using HEPOS data. In the following some representative examples are described.

4.1 RTK field tests

For the RTK field tests, a location in the area of Cyclades islands (point *A*) has been used. As can be seen in Figure 8, the point was chosen close to the boundaries of the area where network solutions are supported (VRS: Virtual Reference Station, MAC: Master Auxiliary Concept, FKP: Area Correction Parameters). The measurements were conducted on five consecutive days (April 12-16, 2012). A total of nine measurement sets has been performed at different times within each day. Each measurement set consisted of consecutive measurements using four different RTK techniques, with the following order:

- Single-base RTK
- VRS using RTCM 2.3
- VRS using RTCM 3.0
- MAC using RTCM 3.1.

The time needed to switch between the four techniques was minimized and did not exceed

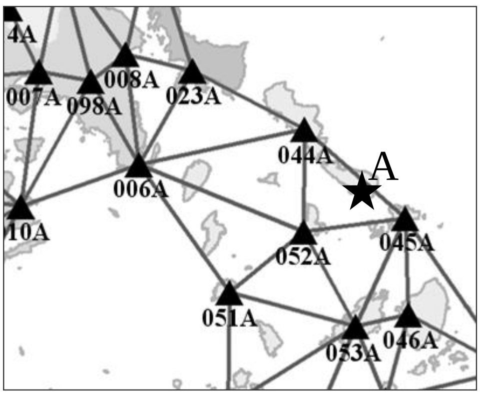

Fig. 8 Location of point *A* (star) where the of the RTK field tests were made. The HEPOS stations are denoted with triangles.

one minute. Thus, we can consider that the measurements of each set refer to the same ionospheric conditions, so they are comparable. All measurements were done using a dual frequency Trimble R6 receiver. The antenna was installed on a building ensuring clear satellite view for elevation angles above 5^{o}.

The main purpose of the field test was to access the impact of ionospheric activity on the initialization time, i.e. the time needed by the RTK rover to resolve the carrier-phase ambiguities (obtain a ‘fixed’ solution). Moreover, the obtained coordinates were checked in order to identify possible wrong fixing, especially when the ionospheric conditions caused delays in fixing the ambiguities. Such problems did not occur; all solutions were reliable.

Figure 9 shows the initialization times for each technique in each measurement set and the hourly I_{95} values of HEPOS for each day of the measurements. The arrows between the upper chart and the I_{95} plots show the particular hourly bars of the I_{95} plots that correspond to the time of each measurement set. As can be seen, most of the measurements were conducted around afternoon, when the ionosphere is mostly charged. Some measurements have been conducted also during night, when sometimes ionospheric instabilities occur (note that the I_{95} plots are given in GPS time, i.e. 3 hours back w.r.t. local time). As can be seen, the majority of the initializations were gained in less than 20 seconds, which is a usual time for fixing within HEPOS. The I_{95} index during these measurement sets varied between 2 and 4 (low to medium ionospheric activity). Quite different results were obtained from the 2^{nd} set of measurements conducted on April 12, 2012 between 20:00 and 21:00 GPT time (23:00 and 00:00 local time). In this case the initialization took over 280 seconds using single-base RTK, about 190s using MAC, about 90s using VRS RTCM2.3 and almost 40s using VRS RTCM3.0. The hourly I_{95} value for the time period of these measurements was above 10, two times higher than the majority of the rest hourly values of that day. Such values occur sometimes in the night as a result of local ionospheric disturbances.

Our field test clearly demonstrated that ionospheric disturbances considerably elongate the initialization time. Furthermore, our test verified that under ionospheric disturbances the network-based techniques are of advantage, as they ensure much shorter initialization times than single-base RTK. Similar results have been presented by

Wanninger (1999) regarding the reliability and accuracy of the VRS technique.

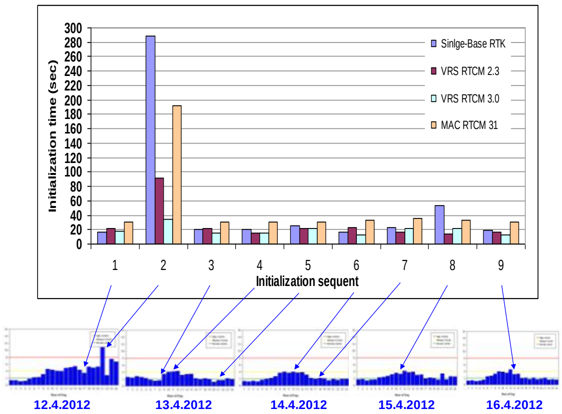

Fig. 9 RTK initialization times obtained at point A (upper chart) and corresponding I_{95} values (lower charts) for April 12-16.

Finally, the use of different RTK techniques in our test allows us to compare the techniques regarding the initialization time on the RTK technique. Table 1 gives the mean initialization time and the associated sigma for each RTK technique computed from all but the 2nd measurement set. This was done in order to compare the techniques under conditions of normal and medium (but not high) ionospheric activity. The VRS technique clearly shows the smallest initialization times, followed by the Single-base and MAC techniques. One would expect that MAC has smaller times than Single-base. In order to investigate this paradox we computed the standard deviation of the initialization time, which is also given in Table 1.

Table 1: Mean initialization time for the RTK techniques used in the field test.

Technique	VRS	VRS	Single-base	MAC
Format	RTCM 3.0	RTCM 2.3	RTCM 2.3	RTCM 3.1
Initial. Time (s)	17	19	24	32
σ of In. time (s)	3.7	3.9	12.1	1.8

Clearly MAC is characterized by the smallest variation in the initialization time. So one could suppose that the algorithm used for MAC needs longer time to fix, but this time is almost constant (ranged between 30s and 35s). Of course, the results of Table 1 refer to conditions of the specific field test and should in no case considered as generally valid. Critical factors that could alter the results are:

- The distance between the rover and the closest reference station. In our test, point *A* was 18 km away from station 045A (see Fig. 8).
- The model of RTK-rover used, as -especially for MAC- the processing engines strongly differ between different rovers.

4.2 Post-processing tests

The ionospheric activity can hardly be predicted on a detailed basis. Ionospheric disturbances can occur suddenly without lasting long, as demonstrated by the 2nd measurement set of the RTK test. Thus, it is very difficult to plan field measurements to investigate such phenomena. In order to overcome this difficulty, post-processing has been used. 1-Hz VRS data have been generated for time periods of high I_{95} values and the initialization time was estimated at the office by post-processing. The VRS data were processed in kinematic mode using Kalman filter algorithms. The GPS processing engine was set-up to process the data only in one direction (only forward) and the time needed to obtain a fixed solution was noted. In this way the operation of an RTK processing engine was simulated. The computations were done using GrafNav ver. 8.40 software package.

In order to verify that our post-processing approach yields similar results as the field measurements, at a first stage we post-processed the same days and times as in the case of the RTK field test. For this purpose 1-Hz VRS data were created for the location of point *A* and for the time periods examined during the field test, i.e April 12 19:00-22:00 GPS time). This interval was processed in a way that the ambiguity search was forced to start every 10 minutes. Thus, for each hour we got six initializations (at hh:00, hh:10, hh:20, hh:30, hh:40 and hh:50). Station 045A at a distance of 18 km from point *A* (see Fig. 8) was used as base station. The number of epochs needed to resolve the ambiguities was examined in connection to the corresponding I_{95} value. For the purpose of extending our test, we also processed the same time interval (19:00-21:00) of the previous and the next day (11 and 13 of April). Figure 10 gives the obtained initialization times and the hourly I_{95} values. As can be seen in the chart for April 12, the initialization times between 20:30 and 21:10 were exceptionally high reaching values up to 283 seconds. These initialization times are is in very good agreement with the initialization times obtained during our field test (see Fig. 9). This consists a first verification of our assumption that post-processing can reveal long initialization times that would have been faced in certain time intervals in the past due to ionospheric activity. The exact initialization time obtained for each initialization trial (every 10 minutes) is given in Table 2.

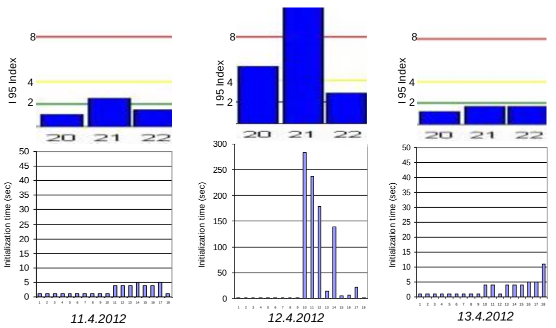

Fig. 10 Hourly I_{95} values (upper charts) and initialization times obtained at point *A* from post-processing (lower charts) for April 11 (left), April 12 (middle) and April 13 (right).

Table 2: Initialization times and I95 values from post-processing of VRS data on point *A* on April 11-13, 2012.

Start time (GPS time)	11.4.2012 Init. time (sec)	I95	12.4.2012 Init. time (sec)	I95	13.4.2012 Init. time (sec)	I95
19:00	1	1.1	1	5.3	1	1.1
19:10	1	1.1	1	5.3	1	1.1
19:20	1	1.1	1	5.3	1	1.1
19:30	1	1.1	1	5.3	1	1.1
19:40	1	1.1	1	5.3	1	1.1
19:50	1	1.1	1	5.3	1	1.1
20:00	1	2.1	1	11.6	1	1.6
20:10	1	2.1	1	11.6	1	1.6
20:20	1	2.1	1	11.6	1	1.6
20:30	1	2.1	283	11.6	4	1.6
20:40	4	2.1	237	11.6	4	1.6
20:50	4	2.1	178	11.6	1	1.6
21:00	4	1.4	14	3.0	4	1.6
21:10	5	1.4	139	3.0	4	1.6
21:20	4	1.4	5	3.0	4	1.6
21:30	4	1.4	6	3.0	5	1.6
21:40	5	1.4	22	3.0	5	1.6
21:50	1	1.4	1	3.0	11	1.6

Looking in more detail at the chart for April 12 (Figure 10) and at Table 2, one can see that:

- although the I_{95} value for 20:00-21:00 of April 12 is high, the delays in fixing took place only after 20:30
- although the I_{95} value for 21:00-22:00 is quite low, the initialization time at 21:10 was relatively high.

This behavior can be well explained, as the I_{95} index in RTK-networks is computed on an hourly basis, while ionospheric disturbances often last shorter. Moreover, one should take into account that the I_{95} index refers to the area of the network in total (not to the location of the user) and that the highest 5% of the ΔI values (equation (1)) are not reflected in I_{95} index.

Post-processing tests have also been performed for the area of Crete. Due to its proximity to the geomagnetic equatorial region, Crete is characterrized by considerably higher I_{95} values compared to the Greek mainland. Because of its long distance from the mainland, Crete is being treated as a separate RTK-network within HEPOS, which means that particular I_{95} indices are computed for Crete based solely on the nine HEPOS stations on the island. For our tests we selected a day of particularly high ionospheric activity, namely the 21^{th} of March 2012. On this day, between 13:00 and 14:00 (GPS time) I_{95} reached 24.6. Two days before, on March 19, the ionospheric activity was dramatically lower, with maximum value limited to 5.1. The daily I_{95} plots for March 19 and 21 are given in Figures 11-12, respectively.

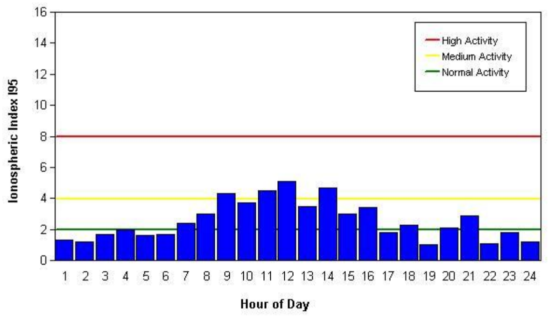

Fig. 11 I_{95} values for Crete on March 19, 2012.

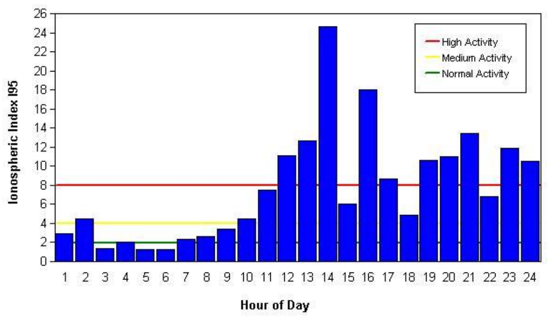

Fig. 12 I_{95} values for Crete on March 21, 2012.

Several tests have been made for different locations in Crete, yielding similar results. A representative example is point *B*, which is shown in Figure 13. 1-Hz VRS data were created for the location of point *B* and for time periods of high ionospheric activity as indicated by the I_{95} index, namely for March 21 14:00-18:00 (GPS time). This interval has been processed in a way that the ambiguity search was forced to start every 10 or 20 minutes. Station 078A at a distance of 25 km from point B (see Fig. 13) was used as base station.

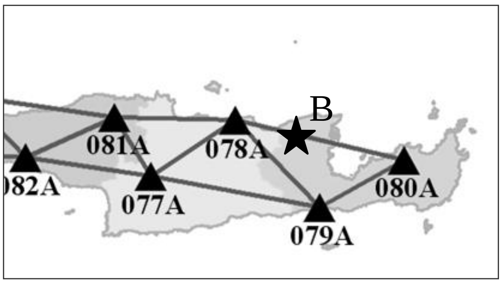

Fig. 13 Location of point *B* on Crete (star) where the PP tests were made. The HEPOS stations are denoted with triangles.

The number of epochs needed to resolve the ambiguities was examined in connection to the corresponding I_{95} value. We also processed the same time interval (14:00-18:00 GPS time) for March 19, a day of moderate ionospheric activity (see Fig. 11). Figure 14 gives the obtained initialization times and the corresponding hourly I_{95} values. The exact initialization time obtained for each initialization trial is given in Table 3. As can be seen, for March 21 the initialization trials that were started at 15:00, 15:20 and 17:00 needed between 26 min and 108 min to yield a fixed solution. As we are interested in RTK applications, we are considering such long times as initialization failures. Looking in more detail at the charts of Figure 14 and at Table 3, we can see that:

- For the 21th of March between 15:00 and 16:00, while I_{95} value was equal to 18, two initialization trials failed and one required 11 minutes to converge to a fixed solution.
- The initialization started at 17:00 of March 21 has failed although the corresponding I_{95} value was relatively low (4.9).
- For the 19th of March (a day of low ionospheric activity) most of the initializations were obtained in about 10 seconds, whereas for the trial started at15:20 more than two minutes were needed although the corresponding I_{95} value was quite low (3.4).

This behavior can be well explained by the reasons mentioned above, for the case of point *A*. Another interesting result can be obtained examining the three initializations started on March 21 between 15:00 and 15:40. The initializations that were started at 15:00 and 15:20 converged to a fixed solution at 16:48 and 16:29, respectively. Thus, the second initialization converged 19 min earlier, although it was started 20 min after the first one. Similarly, the third initialization started at 15:40, although it was started 40 min after the first one, it converged 57 min earlier (at 15:51). This can be attributed to the fact that the processing engine of the used software is based on Kalman filtering (Novatel, 2011). Thus, problematic observations (in our case due to ionospheric conditions) continue to influence the solution even after good observations are again available. The same is valid also for many RTK algorithms, e.g. algorithms that resolve the carrier-phase ambiguities by addition of normal equations.

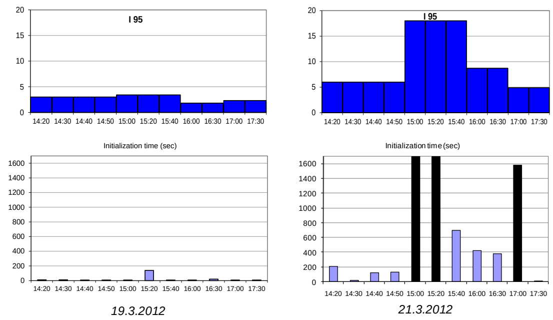

Fig. 14 Hourly I_{95} values (upper charts) and initialization times obtained at point *B* from post-processing (lower charts) for March 19 (left) and March 21 (right) 2012. For clarity, in the lower charts initialization times longer than 1650 s are not shown; black columns correspond to initialization failures.

Table 3: Initialization times and I_{95} values from post-processing of VRS data on point B on March 19 and 21, 2012.

Start time (GPS time)	**19.3.2012**		**21.3.2012**	
	Init. time (sec)	**I95**	**Init. time** (sec)	**I95**
14:20	11	3.0	207	6.0
14:30	10	3.0	18	6.0
14:40	8	3.0	122	6.0
14:50	8	3.0	128	6.0
15:00	8	3.4	6523 *	18.0
15:20	139	3.4	5349 *	18.0
15:40	8	3.4	696	18.0
16:00	8	1.8	422	8.7
16:30	20	1.8	377	8.7
17:00	8	2.3	1580 *	4.9
17:30	8	2.3	8	4.9

(*): For RTK purposes considered as Initialization Failures

5 Conclusions

Our RTK and post-processing tests confirmed the difficulties in obtaining a fixed solution caused by the ionospheric activity as we are approaching the maximum of the 24th solar cycle. These difficulties are expected to become more intense next year, as the maximum of the current solar cycle has not yet been reached.

The RTK tests demonstrated that the initialization time on a certain location can change dramatically with time, not only from day to day but also from hour to hour within the same day depending on the ionospheric conditions. The index I_{95} proved to be very helpful for GPS users in order to identify unfavorable ionospheric conditions.

Finally, we showed that using post-processing in kinematic mode, we can effectively identify time periods in the past when RTK fixing would have been difficult due to intense ionospheric activity.

Acknowledgments

The HEPOS project is part of the Operational Program "Information Society" and is co-funded by the European Regional Development Fund.

References

Chen, X., Landau, H., Vollath, U. (2003). New Tools for Network RTK Integrity Monitoring. *Proceedings of the 16th International Technical Meeting of the Satellite Division of The Institute of Navigation (ION GPS/GNSS 2003), Portland OR,* pp. 1355-1360.

Hofmann-Wellenhof, B., H. Lichtenegger and E.Wasle (2008). GNSS–global navigation satellite systems: GPS, GLONASS, Galileo, and more. Springer Verlag.

Liu L B, Wan W X, Chen Y D, et al. (2011). Solar activity effects of the ionosphere: A brief review. *Chinese Sci Bull, 2011, 56: 1202−1211, doi*: 10. 1007/s11434-010-4226-9

Novatel. GrafNav / GrafNet User Guide. http://www.novatel.com/assets/Documents/Waypoint/Downloads/NavNet840_Manual.pdf, 2011.

Schaer, S., Beutler, G., Rothacher, M. (1998). Mapping and predicting the ionosphere. *Proceedings of the IGS AC Workshop, Darmstadt, Germany*, (pp. 9-11).

Schaer, S. (1999). Mapping and predicting the Earth's ionosphere using the Global Positioning System, *228 pp., PhD thesis, Astronomical Institute, University of Bern, Bern, Switzerland.*

Trimble Navigation Ltd (2008). Trimble GPSNet VRS Software User guide. Version 2.70. Dayton, Ohio, USA.

Wanninger, L. (1999). The Performance of Virtual Reference Stations in Active Geodetic GPS-Networks under Solar Maximum Conditions. *Proceedings of the 12th International Technical Meeting of the Satellite Division of The Institute of Navigation (ION GPS 99), Nashville TN*, 1419-1427.

Wanninger, L. (2004). Ionospheric disturbance indices for RTK and network RTK positioning. *Proceedings of the National Technical Meeting of the Satellite Division of the Institute of Navigation, ION GPS 2004 September 2004, Long Beach, USA*, pp. 2849-2854.

Warnant, R., Grevesse, J., & Pottiaux, E. (2003). Processing GPS measurements during periods of high ionospheric activity: the influence on GPS data preprocessing. *Report on the Symposium of the IAG Subcommission for Europe (EUREF) Held in Ponta Delgada, 5-8 June 2002,* Issue 12: 365-368, Verlag des Bundesamtes für Kartographie und Geodäsie.